Heralded Generation of an Atomic NOON State

Yu-Ao Chen,[1,2] Xiao-Hui Bao,[1,2] Zhen-Sheng Yuan,[1,2] Shuai Chen,[1,2] Bo Zhao,[1] and Jian-Wei Pan[1,2]

[1]*Physikalisches Institut, Ruprecht-Karls-Universität Heidelberg, Philosophenweg 12, 69120 Heidelberg, Germany*
[2]*Hefei National Laboratory for Physical Sciences at Microscale and Department of Modern Physics, University of Science and Technology of China, Hefei, Anhui 230026, China*

(Received 31 August 2009; published 26 January 2010)

We report the heralded generation of an atomic NOON state by observation of phase super resolution in a motion-sensitive spin-wave (SW) interferometer. The SW interferometer is implemented by generating a superposition of two SWs and observing the interference between them, where the interference fringe is sensitive to the atomic collective motion. By heralded generation of a second order NOON state in the SW interferometer, we observe the interference pattern which provides strong evidence of phase super resolution. The demonstrated SW interferometer can in principle be scaled up to a highly entangled state, and thus is of fundamental importance, and might be used as an inertial sensor.

DOI: 10.1103/PhysRevLett.104.043601 PACS numbers: 42.50.Dv, 03.75.Dg, 06.30.Gv, 37.25.+k

The optical interferometer [1] and the atom interferometer [2] have become essential tools for measuring position, displacement, or acceleration. In these devices, a light pulse or the wave packet of neutral atoms in an ensemble are coherently split and recombined in space or time domain by applying mechanical or optical gratings. The gravity or platform rotation will cause a motion-sensitive phase shift, which can be measured from the interference fringes.

As is well known, by exploiting suitable quantum entanglement, e.g., a NOON state [$|\mathrm{NOON}\rangle = \frac{1}{\sqrt{2}}(|N\rangle_a|0\rangle_b + |0\rangle_a|N\rangle_b)$, which denotes the N-particle entanglement in a Fock state basis] or a Greenberger-Horne-Zeilinger (GHZ) state [$|\mathrm{GHZ}\rangle = \frac{1}{\sqrt{2}}(|1\rangle_{a_1}|0\rangle_{b_1}\ldots|1\rangle_{a_N}|0\rangle_{b_N} + |0\rangle_{a_1}|1\rangle_{b_1}\ldots|0\rangle_{a_N}|1\rangle_{b_N})$, which denotes the N-particle entanglement in qubit basis], the measurement precision can be improved [1,3]. For optical interferometers, the principle of the quantum enhanced measurement has been demonstrated by exploiting photonic NOON state, where phase super resolution [4–6] and phase super sensitivity [7] have been observed. However, generating atomic NOON state or GHZ state and exploiting them in atom interferometers are still challenging for current technology.

Here, we demonstrate a heralded generation of an atomic NOON state in a motion-sensitive SW interferometer. The SW is a collective state in a cold atomic ensemble, which is created by applying a classical pulse to the atoms to induce spontaneous Raman scattering and detecting the emitted Stokes photon [8]. The SW interferometer is implemented by exploiting the superposition of the modes of the SW. By applying a radiation pressure force, the collective motion of the atoms is introduced, which will cause a phase shift. This phase shift is sensitive to the collective motion and can be measured by applying a classical light to convert the superposition of collective states into a superposition of anti-Stokes photons [9]. With a second order NOON state in the SW interferometer generated by registering the two photon events, the interference fringe provides strong evidence of phase super resolution. Our method can lead to phase super sensitivity with the improvement of coherence time of the SWs. Moreover, the SW interferometer can in principle be scaled up to highly entangled states, which might be useful in inertial sensing.

To illustrate the working scheme of SW interferometer, we consider a cold atomic cloud with the Λ-type level structure shown in the Fig. 1. About 10^6 atoms are initially optically pumped to $|g\rangle$. An off-resonant σ^- polarized write pulse coupling the transition $|g\rangle \to |e\rangle$ with wave vector $\mathbf{k}_W$ is applied to the atomic ensemble along the axial direction, inducing spontaneous Raman scattering. Two Stokes fields with σ^- polarization and wave vector $\mathbf{k}_{Sa}$ and $\mathbf{k}_{Sb}$ are collected at an angle of $\theta_{a,b} = \pm\theta$ relative to the write beam. The atom-light field in each mode can be expressed as [8] $|\Psi\rangle_i \sim |0\rangle_i^S|0\rangle_i + \sqrt{\chi_i}|1\rangle_i^S|1\rangle_i + \chi_i|2\rangle_i^S|2\rangle_i + O(\chi_i^{3/2})$, where $\chi_a = \chi_b \ll 1$ is the excitation probability of one collective spin excitation in mode i ($i = a,\, b$), $|j\rangle_i^S$ denotes the Stokes field S_i with photon number j, while $|j\rangle_i = S_i^{\dagger j}|0\rangle_i$ denotes the j-fold collective spin excitation in mode i, with $|0\rangle_i = \bigotimes_l |g\rangle_l$ the vacuum, $S_i^\dagger = \frac{1}{\sqrt{M_i}}\sum_l e^{i\Delta\mathbf{k}_i\cdot\mathbf{r}_l^i}|s\rangle_l\langle g|$ the creation operator of SW_i, where $\Delta\mathbf{k}_i = \mathbf{k}_W - \mathbf{k}_{Si} \simeq \mathbf{k}_W \sin\theta_i$ is the wave vector of SW_i, and $\mathbf{r}_l^i$ the coordinate of the l-th atom in mode i.

The two Stokes fields are rotated to be horizontally ($|H\rangle$) and vertically ($|V\rangle$) polarized for mode a and b, respectively, and are combined on a polarized beam splitter (PBS). The half-wave plate (HWP_s) is set to 22.5° to measure the Stokes photons under $|\pm\rangle = \frac{1}{\sqrt{2}}(|H\rangle \pm |V\rangle)$ basis. Neglecting high order excitations, a click on detector D_{S1} or D_{S2} will project the atomic ensembles into the superposition state

$$|\Psi\rangle = \frac{1}{\sqrt{2}}(|1\rangle_a|0\rangle_b \pm |0\rangle_a|1\rangle_b). \quad (1)$$

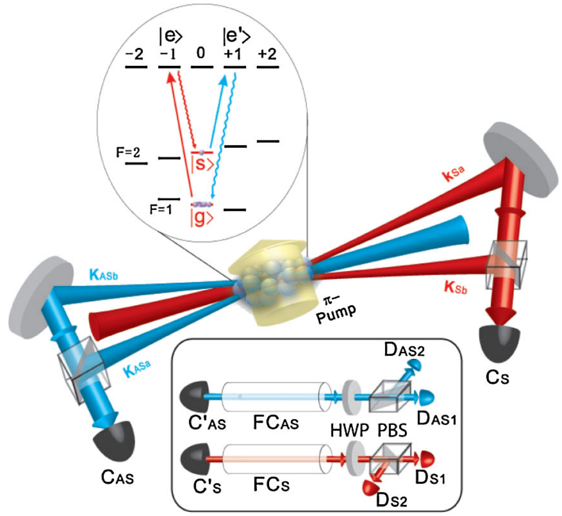

FIG. 1 (color online). Experimental setup of the SW interferometer. The inset at the top shows the relevant Zeeman levels for the $|5S_{1/2}\rangle \to |5P_{1/2}, F' = 2\rangle$ transition of ^{87}Rb atoms. Before the experimental cycles, we optically pump the atoms in $|g\rangle$ by applying two pumping lights (see [11]), one of which is shining in from the lateral side (π-pump) to introduce radiation pressure force. A weak σ^- polarized write pulse is applied to generate two modes of SW and Stokes fields via spontaneous Raman transition $|g\rangle \to |e\rangle \to |s\rangle$. The Stokes fields are collected at the angle of $\pm 0.6°$ relative to the write beam, combined on a PBS, and directed into a single mode fiber via a fiber coupler (C_S). After a controllable delay, a strong σ^+ polarized read beam induces the transition $|s\rangle \to |e'\rangle \to |g\rangle$, converting the two SWs into two anti-Stokes fields, which are overlapped in another PBS and then directed to a coupler (C_{AS}). Passing through two filter cells (FC), respectively, the anti-Stokes photon from C'_{AS} and Stokes photon from C'_S are then sent to the polarization analyzers combined with half wave plate (HWP), polarized-beam splitter (PBS), and single photon detectors (D), as illustrated in the inset at bottom. Filter cells are properly pumped in order to absorb the remaining leakage from read or write beams while being transparent for the signals.

Such a SW superposition state can be exploited to implement the Mach-Zehnder interferometer.

Assume the atoms undergo a collective motion, e.g., motion caused by gravitational acceleration, described as $\mathbf{r}'^i_l = \mathbf{r}^i_l + \mathbf{r}_c$. Since $|1\rangle_i = S_i^\dagger|0\rangle_i = \frac{1}{\sqrt{M_i}}\sum_l e^{i\Delta\mathbf{k}\cdot\mathbf{r}^i_l}|g\ldots s_l\ldots g\rangle$, after the collective motion the SW will change to $|1'\rangle_i = e^{i\phi_i}|1\rangle_i$ with $\phi_i = \Delta\mathbf{k}_i \cdot \mathbf{r}_c$, where $\Delta\mathbf{k}_a = -\Delta\mathbf{k}_b \equiv \Delta\mathbf{k}$. Thereby, we obtain

$$|\Psi'\rangle \sim \frac{1}{\sqrt{2}}(|1\rangle_a|0\rangle_b \pm e^{-i2\Delta\phi}|0\rangle_a|1\rangle_b), \qquad (2)$$

with $\Delta\phi = \Delta\mathbf{k}\cdot\mathbf{r}_c$. It can be readily seen that the collective motion of the atoms is mapped to a relative phase in the superposition state. This phase and thus the collective motion can be measured by converting the SW back into photons and observing the interference pattern. In this way, if $\Delta\mathbf{k}$ is set in the direction of the gravity, one can measure the gravitational acceleration. The measurement precision is corresponding to the sensitivity of the interferometer determined by length of the wave vector $\Delta\mathbf{k}$, which is controllable in practice.

Such a single-excitation SW interferometer can be looked upon as the first order of a NOON state [10]. Higher order NOON state can be generated in a heralded way by using the linear optical methods (see supplementary material [11] for detail), described as $|\mathrm{NOON}\rangle = \frac{1}{\sqrt{2}}(|N\rangle_a|0\rangle_b + |0\rangle_a|N\rangle_b)$, where $|N\rangle_i = \frac{1}{\sqrt{N!}}S_i^{\dagger N}|0\rangle_i$ denotes the N-fold excitation in mode i ($i = a, b$). Thus, the collective motion of the atoms will induce a phase as $|\mathrm{NOON}'\rangle \sim \frac{1}{\sqrt{2}}(|N\rangle_a|0\rangle_b + e^{-i2N\Delta\phi}|0\rangle_a|N\rangle_b)$. Note that, although the method is in principle extendable [4] to arbitrary N, the efficiency of generating the desired NOON state drops off exponentially [10] with N. In order to be more efficient in employing entanglement, one can exploit multiple atomic ensembles to prepare an N-quanta GHZ state [12], which can be deterministically generated in a scalable way [13,14] and share the same sensitivity as a NOON state (see [11] for details). Therefore, the SW interferometer would be N times more sensitive to the motion with the help of these highly entangled states and thus can be exploited to demonstrate the phase super-resolution and phase super sensitivity.

Demonstration of the SW interferometer critically depends on the coherence time of the SW excitation. In the experiment, we implement the SW interferometer with ^{87}Rb atoms trapped in a magneto-optical trap at a temperature of about 100 μK. By exploiting the clock transitions of $|g\rangle = |5S_{1/2}, F = 1, m_F = 0\rangle$ and $|s\rangle = |5S_{1/2}, F = 2, m_F = 0\rangle$ as the two ground states to avoid the deleterious effects induced by magnetic field, e.g., Larmor precession or inhomogeneous broadening, we achieve the coherence time of the SW of about 200 μs, which is limited by the dephasing of the SW induced by atomic random motion [15]. With such a coherence time, it is now possible to study the motion sensitivity of the SW interferometer. With our setup, we obtain a typical generation probability for the SW superposition state (1) of about 300 per second.

To show the motion sensitivity, we introduce a collective motion during the pumping stage, where the atoms absorb photons from the π-pump light and the $2 \to 2$ pump, and then decay spontaneously (see [11] for details). Since the $2 \to 2$ pump is shined with the cooler light from six directions, and spontaneous emission is in arbitrary directions, on average they give no contribution to the collective motion. While the π-pump light from the lateral side acts as a pushing laser, which causes a radiation pressure force and accelerates the atoms [16] until they are pumped to $|g\rangle$. We denote the velocity acquired in this process by $\mathbf{v_p} = v_p\hat{\mathbf{e}}_p$. Besides, the unbalance of other lasers, i.e., cooler, repumper, and, etc., will also induce an initial velocity $\mathbf{v_0}$ when the atoms are released. Therefore, the generated superposition state $|\Psi\rangle$ [Eq. (1)] will evolve to $|\Psi'\rangle$ [Eq. (2)] after a free evolution time of δt, where $\Delta\phi = \Delta\phi(\delta t) = \Delta\mathbf{k}\cdot\mathbf{v_c}\delta t$ with $\mathbf{v_c} = \mathbf{v}_p + \mathbf{v_0}$ and in which the atomic random motion is neglected.

To measure $\Delta\phi(\delta t)$, a strong σ^+ polarized read light, coupling the transition $|e'\rangle \rightarrow |g\rangle$, counter-propagating with the write light, converts the collective excitations into σ^+ polarized anti-Stokes fields. The anti-Stokes fields from two atomic ensembles are rotated to be perpendicular to each other and combined on a PBS (Fig. 1), which can be described by $|\Psi\rangle_{\rm AS} \sim \frac{1}{\sqrt{2}}(|H\rangle_{\rm AS} \pm e^{-i[2\Delta\phi(\delta t)]}e^{i(\phi_1+\phi_2)}|V\rangle_{\rm AS})$, where ϕ_1 (ϕ_2) represents the propagating phase difference between two Stokes (anti-Stokes) fields before overlapping. In the experiment, the total phase $\phi_1 + \phi_2$ is actively stabilized and set to a fixed value [17]. The interference pattern is observed by setting the $\mathrm{HWP_{AS}}$ at 22.5° to detect the anti-Stokes fields under $|+\rangle/|-\rangle$ basis. The experiment results are shown in Fig. 2. We change the power of the π pump and measure the fidelity of anti-Stokes field on $|+\rangle$ as a function of δt, on condition of a click of Stokes field on state $|+\rangle$ (solid circles) and $|-\rangle$ (open circles). The collective motion velocity can be obtained from the period of the interference pattern $T = \frac{\pi}{\Delta\mathbf{k}\cdot\mathbf{v_c}}$, which varies from 300 to 1200 μs.

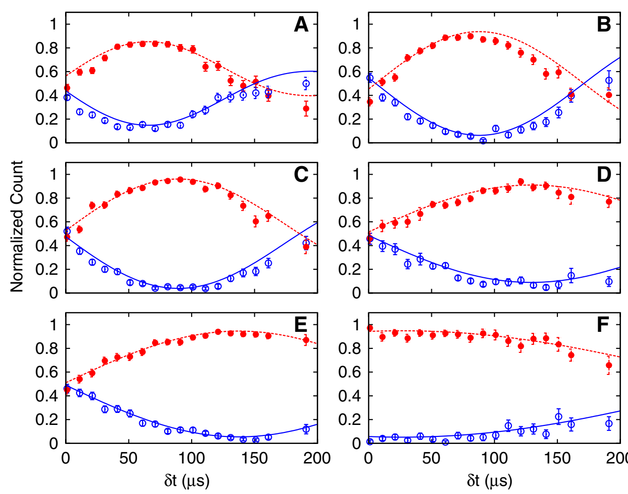

FIG. 2 (color online). The fidelity of anti-Stokes field on $|+\rangle$ as a function of δt. Solid circles (open circles) represents the measured fidelity of anti-Stokes field on $|+\rangle$ on condition of a click of Stokes field on state $|+\rangle$ ($|-\rangle$). The power of the π-Pump is: (a) 6 mW, (b) 4.5 mW, (c) 3 mW, (d) 1.5 mW, (e) 0.75 mW, (f) 0 mW. The experimental data are jointly fitted by using $f_{+|+}(\delta t) = [0.5 + a\sin^2(\pi\frac{\delta t}{T} + \phi_0)e^{-\delta t^2/\tau^2}]/(1 + ae^{-\delta t^2/\tau^2})$ and $f_{+|-}(\delta t) = [0.5 + a\cos^2(\pi\frac{\delta t}{T} + \phi_0)e^{-\delta t^2/\tau^2}]/(1 + ae^{-\delta t^2/\tau^2})$ (see [11] for detail). The evolution period $T = \frac{\pi}{\Delta\mathbf{k}\cdot\mathbf{v_c}}$ is measured to be (a) 317 ± 18 μs, (b) 330 ± 15 μs, (c) 378 ± 14 μs, (d) 555 ± 47 μs, (e) 591 ± 30 μs, (f) 1177 ± 152 μs. Error bars represent statistical errors, which are ± 1 s.d.

The velocity that the atoms acquired as a function of the π-pump power is shown in Fig. 3. One can see that the average velocity will first increase with the π-pump power, and reach a plateau when the π-pump is sufficiently strong. This might be related with the pumping efficiency in the pumping stage, since when all the atoms are pumped to the $|g\rangle$, the atoms will not absorb photons from π-pump any more. Note that the population in other Zeeman sublevels arising from insufficient pumping will not affect the interference pattern since the decoherence time in other states is very short (about microseconds) due to inhomogeneous broadening.

To demonstrate the advantage of quantum entanglement, we generate the second order NOON state, which can be described as $|\Psi\rangle_{\rm NOON} = \frac{1}{\sqrt{2}}(|2\rangle_a|0\rangle_b - |0\rangle_a|2\rangle_b)$. This is achieved with the help of a feedback circuit [18] by registering the coincidence count between single photon detectors D_{S1} and D_{S2}, with a typical generation probability of 1 per second. Note that the noise in preparing the NOON state is negligible (see [11] for details). After a free evolution time of δt, we have $|\Psi\rangle_{\rm NOON'} \sim \frac{1}{\sqrt{2}}(|2\rangle_a|0\rangle_b - e^{-i[4\Delta\phi(\delta t)]}|0\rangle_a|2\rangle_b)$. By converting the second order state to anti-Stokes fields and measuring the coincidence count between detectors $D_{\rm AS1}$ and $D_{\rm AS2}$, we obtain the phase $\Delta\phi(\delta t)$. The coincidence count per successful generation of a NOON state event is shown in Fig. 4(a). For comparison, we give the interference fringe for the first order NOON state under the same condition as shown in Fig. 4(b), which is taken directly after the measurement of the second order interference pattern. One can see that interference fringes for $N = 2$ state oscillate about twice faster than that of $N = 1$, which provides strong evidence of phase super resolution. Besides, the interference fringe for $N = 2$ also decays faster than $N = 1$, since NOON state is also sensitive to decoherence [1]. The $N = 2$ data are fitted using a model by taking into account both the

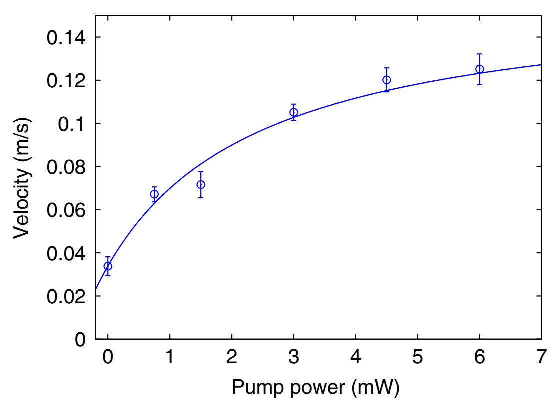

FIG. 3 (color online). The atomic velocity as a function of the π-pump power. The initial velocity induced by the unbalance of other lasers is about 0.03 m/s. The velocity acquired in the pumping stage increases with the pumping power until reaching a plateau of about 0.12 m/s. Error bars represent statistical errors, which are ± 1 s.d.

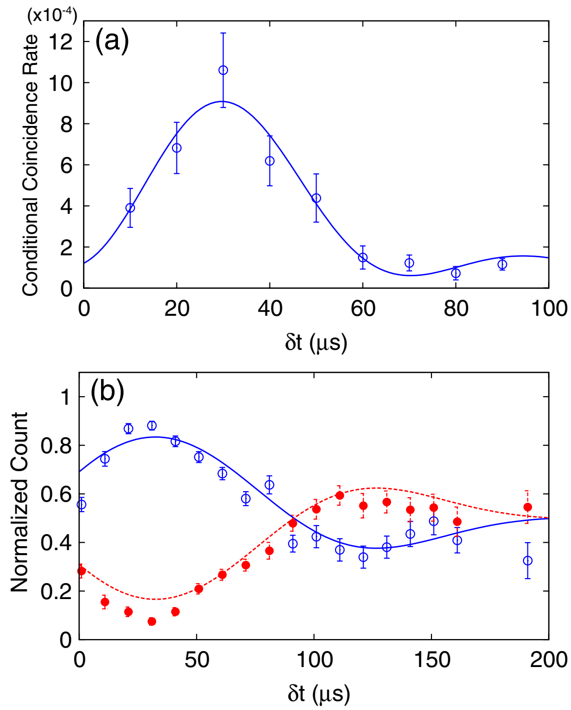

FIG. 4 (color online). Comparison of the performance of the first and second order NOON state. (a) The normalized coincidence count for the second order NOON state as a function of δt. The experimental data are fitted by using $c(\delta t) = b\sin^2(\pi\frac{\delta t}{T'} + \phi_0')e^{-2\delta t^2/\tau^2} + de^{-\delta t^2/\tau^2}$. The optimization fitting gives an evolution period of $T' = (73 \pm 7)$ μs (See [11] for details). (b) The interference pattern for $N = 1$ under the same condition. The lines are the fitted with the same method as in Fig. 2. The fitting evolution period is $T = (220 \pm 17)$ μs. Error bars represent statistical errors, which are ± 1 s.d.

oscillation and decoherence, where the parameters are determined by optimizing the reduced chi-square (see [11] for details). The fitting gives an evolution period of $T' = (73 \pm 7)$ μs for $N = 2$, which is slightly shorter than half of $T = (220 \pm 17)$ μs for $N = 1$. This is mainly because that due to decoherence, we can not observe more than one evolution period, and some imperfections in experiment such as the drifting of the laser power and drifting of the coupling between different channels will contribute errors to the signal. Note that the data in Fig. 4 are taken under π-pump power of 6 mW. There is a slight change of the initial velocity of the atomic ensemble compared to the original condition, which makes the first order evolving period slightly different from the one given in Fig. 2(a).

With emphasis, we note that the NOON state is not only more sensitive to the collective motion, but also more sensitive to decoherence [1,19]. Therefore, to achieve phase super sensitivity, the coherence time of the NOON state has to be much larger than its free evolution time [20,21]. However, in our experiment, since the coherence time is comparable to the free evolution time, the gain obtained by using $N = 2$ NOON state is partially offset by the corresponding faster decoherence, and thus we failed to achieve phase super sensitivity. It is expected that our NOON state will show the desired phase super sensitivity with the improvement of the coherence time.

In summary, we have demonstrated a heralded atomic NOON state in a SW interferometer. In the experiment, the second order NOON state is generated, which provides strong evidence of phase super resolution. A higher order SW NOON state with small $N = 4$ or 5 can be generated in the current setup to further demonstrate the principle of quantum enhanced measurement. Besides, since the quantum memory is automatically built into our system, the N-quanta SW GHZ state can be deterministically generated in a scalable way, which is a distinct advantage compared with photonic entanglement. Thus, the SW interferometer might be used as an inertial sensor.

This work was supported by the European Commission through the ERC Grant and the STREP project HIP, the National Fundamental Research Program (Grant No. 2006CB921900), the CAS, and the NNSFC.

[1] J. P. Dowling, Contemp. Phys. **49**, 125 (2008).
[2] A. D. Cronin, J. Schmiedmayer, and D. E. Pritchard, Rev. Mod. Phys. **81**, 1051 (2009).
[3] V. Giovannetti, S. Lloyd, and L. Maccone, Science **306**, 1330 (2004).
[4] P. Walther *et al.*, Nature (London) **429**, 158 (2004).
[5] M. Mitchell, J. Lundeen, and A. Steinberg, Nature (London) **429**, 161 (2004).
[6] K. J. Resch *et al.*, Phys. Rev. Lett. **98**, 223601 (2007).
[7] T. Nagata *et al.*, Science **316**, 726 (2007).
[8] L.-M. Duan, M. D. Lukin, J. I. Cirac, and P. Zoller, Nature (London) **414**, 413 (2001).
[9] M. D. Eisaman *et al.*, Nature (London) **438**, 837 (2005).
[10] P. Kok, H. Lee, and J. P. Dowling, Phys. Rev. A **65**, 052104 (2002).
[11] See supplementary material at http://link.aps.org/supplemental/10.1103/PhysRevLett.104.043601.
[12] D. Greenberger, M. Horne, and A. Zeilinger, *Bell's Theorem, Quantum Theory, and Conceptions of the Universe* (Kluwer, Dordrecht, 1989), Vol. 69.
[13] S. D. Barrett, P. P. Rohde, and T. M. Stace, arXiv:0804.0962v1.
[14] D. E. Browne and T. Rudolph, Phys. Rev. Lett. **95**, 010501 (2005).
[15] B. Zhao *et al.*, Nature Phys. **5**, 95 (2009).
[16] W. Wohlleben, F. Chevy, K. Madison, and J. Dalibard, Eur. Phys. J. D **15**, 237 (2001).
[17] Y.-A. Chen *et al.*, Nature Phys. **4**, 103 (2008).
[18] S. Chen *et al.*, Phys. Rev. Lett. **97**, 173004 (2006).
[19] S. F. Huelga *et al.*, Phys. Rev. Lett. **79**, 3865 (1997).
[20] M. Auzinsh *et al.*, Phys. Rev. Lett. **93**, 173002 (2004).
[21] D. Leibfried *et al.*, Science **304**, 1476 (2004).